

# 1 The spatiotemporal dynamics of recognition memory for complex versus

## 2 simple auditory sequences

4 Fernández Rubio, G.<sup>1,2\*</sup>, Brattico, E.<sup>1,3</sup>, Kotz, S. A.<sup>2</sup>, Kringselbach, M. L.<sup>1,4,5</sup>, Vuust, P.<sup>1</sup>,  
5 Bonetti, L.<sup>1,4,5</sup>

6

7

<sup>8</sup> *<sup>1</sup>Center for Music in the Brain, Department of Clinical Medicine, Aarhus University & The Royal Academy of*  
*<sup>9</sup> Music, Aarhus, Aalborg, Denmark*

10 *<sup>2</sup>Department of Neuropsychology and Psychopharmacology, Faculty of Psychology and Neuroscience,*  
11 *Maastricht University, Maastricht, The Netherlands*

<sup>12</sup>*Department of Education, Psychology, Communication, University of Bari Aldo Moro, Bari, Italy*

13 <sup>4</sup>Centre for Eudaimonia and Human Flourishing, University of Oxford, Oxford, United Kingdom

14 <sup>5</sup>*Department of Psychiatry, University of Oxford, Oxford, United Kingdom*

15

16

17 \*Corresponding author: [gemmafr@clin.au.dk](mailto:gemmafr@clin.au.dk)

18 **Abstract**

19 Differently from visual recognition, auditory recognition is a process relying on the  
20 organization of single elements that evolve in time. Here, we aimed to discover the  
21 spatiotemporal dynamics of this cognitive function by adopting a novel strategy for varying  
22 the complexity of musical sequences. We selected traditional tonal musical sequences and  
23 altered the distance between pitches to obtain matched atonal sequences. We then recorded  
24 the brain activity of 71 participants using magnetoencephalography (MEG) while they  
25 listened to and later recognized auditory sequences constructed according to simple (tonal) or  
26 complex (atonal) conventions. Results reveal qualitative changes in neural activity dependent  
27 on stimulus complexity: recognition of tonal sequences engaged hippocampal and cingulate  
28 areas, whereas recognition of atonal sequences mainly activated the auditory processing  
29 network. Our findings highlight the involvement of a cortico-subcortical brain network for  
30 auditory recognition and support the idea that stimulus complexity qualitatively alters the  
31 neural pathways of recognition memory.

32

33 **Keywords**

34 Recognition memory, Stimulus complexity, Predictive coding of music (PCM),  
35 Magnetoencephalography (MEG)

36 ***Introduction***

37 Encoding and recognizing sounds that are structurally complex is a cognitive challenge  
38 relying on neural mechanisms that are not yet fully elucidated. To memorize complex sound  
39 sequences, we likely depend on the temporal organization of a stimulus' components and  
40 memory functions<sup>1</sup>.

41 Memory encoding takes place in the hippocampus<sup>2-4</sup>, whereas subsequent processes  
42 related to recognition memory are supported by a functional network of interconnected  
43 regions in the medial temporal lobe, including the hippocampus, insula, and inferior temporal  
44 cortex<sup>2, 5, 6</sup>. For memory consolidation, communication between hippocampal and  
45 neocortical areas is needed<sup>7-9</sup>. Much evidence comes from studies using static visual stimuli,  
46 such as pictures of objects, faces, or natural scenes<sup>10-12</sup>. In audition, however, information  
47 and meaning unfold over time as the brain attempts to predict upcoming stimuli based on  
48 prior memory representations. Hence, to better understand memory recognition and its  
49 underlying fast brain dynamics, novel methods must be adopted that highlight the temporal  
50 properties of dynamic stimuli. This can be done by studying the neural activity underlying the  
51 processing of sound sequences that acquire meaning through their evolution over time, such  
52 as music<sup>13-15</sup>.

53 According to the predictive coding of music (PCM) theory, music processing is bound  
54 by hierarchical Bayesian rules, wherein the brain compares musical information with its  
55 internal predictive model in an attempt to reduce a prediction error<sup>16-19</sup>. Specifically, bottom-  
56 up sensations evoked by auditory stimuli are processed in primary cortices and contrasted  
57 with top-down predictions in higher-order cortices to generate musical expectations and  
58 minimize hierarchical prediction errors<sup>19-21</sup>. Predictive mechanisms rely on long- and short-  
59 term memory functions, familiarity, and listening strategies to create musical expectations<sup>18</sup>.  
60 Overall, the PCM model provides a reliable framework for studying music perception<sup>22-25</sup>,  
61 training<sup>26, 27</sup>, action<sup>28, 29</sup>, synchronization<sup>30-32</sup>, and emotion<sup>33-35</sup>. In recent years, studies  
62 have also began exploring the neural underpinnings of musical memory. Using functional  
63 resonance imaging (fMRI) and a naturalistic music listening paradigm, Alluri et al.<sup>36</sup>  
64 investigated the neural correlates of music processing and reported activation of cognitive,  
65 motor, and limbic brain networks for the continuous processing of timbral, tonal, and  
66 rhythmic features. Subsequently, using the same stimuli, Burunat et al.<sup>37</sup> reported the  
67 recruitment of memory-related and motor brain regions during the recognition of musical

68 motifs. Despite their contributions, these studies fail to identify the fine-grained temporal  
69 mechanisms of sound encoding and memory processes.

70 More recently, we introduced novel applications of magnetoencephalography (MEG)  
71 combined with magnetic resonance imaging (MRI) to study music recognition. These studies  
72 accentuated the temporal involvement of a widespread cortico-subcortical brain network  
73 comprising the primary auditory cortex, superior temporal gyrus, frontal operculum,  
74 cingulate gyrus, orbitofrontal cortex, and hippocampus during recognition of auditory  
75 (musical) sequences <sup>38-40</sup>. Overall, these investigations have provided unique insight into the  
76 neural mechanisms underlying the recognition of temporal sequences. What remains to be  
77 addressed is how these mechanisms are modulated by stimulus complexity.

78 Here, we used melodic sequences, where meaning emerged from the sequential  
79 combination of individual tones over time <sup>40</sup>, and varied the tone distribution to obtain new,  
80 complex musical sequences. In this scenario, encoding and recognition of the musical  
81 sequences largely depend on the sequential order of the tones that comprise it. We first  
82 selected musical sequences based on the rules of tonality, which is the dominant musical  
83 system in Western popular music <sup>41</sup>. Second, by modifying the tone intervals (i.e., the  
84 distances between pitches) while keeping all other variables (e.g., rhythm, tempo, timbre)  
85 constant, we generated matched *atonal* musical sequences. The stimulus manipulation was  
86 based on previous literature, which reported that tonal rather than atonal musical sequences  
87 are overall easier to process <sup>42-46</sup> and more appreciated by non-expert listeners <sup>46-48</sup>. Unlike  
88 tonal music, atonal music is characterized by the absence of a clear tonal center and  
89 hierarchical stability, which significantly reduces its predictive value and gives rise to  
90 increased prediction errors <sup>42-45, 49</sup>. Thus, we expected that the alteration of tonal intervals  
91 would reduce the predictability of the atonal sequences, leading to increased difficulty to  
92 recognize them.

93 To summarize, in the current study we used magnetoencephalography (MEG) and a  
94 musical recognition task <sup>38-40</sup> while participants listened to and recognized auditory (musical)  
95 sequences of varying complexity. We aimed at describing its fine-grained spatiotemporal  
96 dynamics. Following previous studies <sup>36-40</sup>, we expected that the recognition of auditory  
97 sequences would activate a widespread brain network that includes both auditory (e.g.,  
98 primary auditory cortex, superior temporal gyrus, Heschl's gyrus, planum temporale, insula)  
99 and memory processing areas (e.g., hippocampus, cingulate gyrus). We further hypothesized  
100 that neural activity would be distributed along two main frequency bands that reflected the  
101 occurrence of two different cognitive processes: a slow frequency band related to the

102 recognition of the full musical sequence in memory processing areas, and a fast frequency  
103 band associated with the processing of each individual tone of the musical sequence in  
104 auditory regions. More importantly, we hypothesized that, based on stimulus complexity,  
105 tonal music would be more efficiently processed than atonal music, which would be reflected  
106 in different behavioral responses and distinct neural pathways during recognition of tonal and  
107 atonal sequences.

108 **Results**

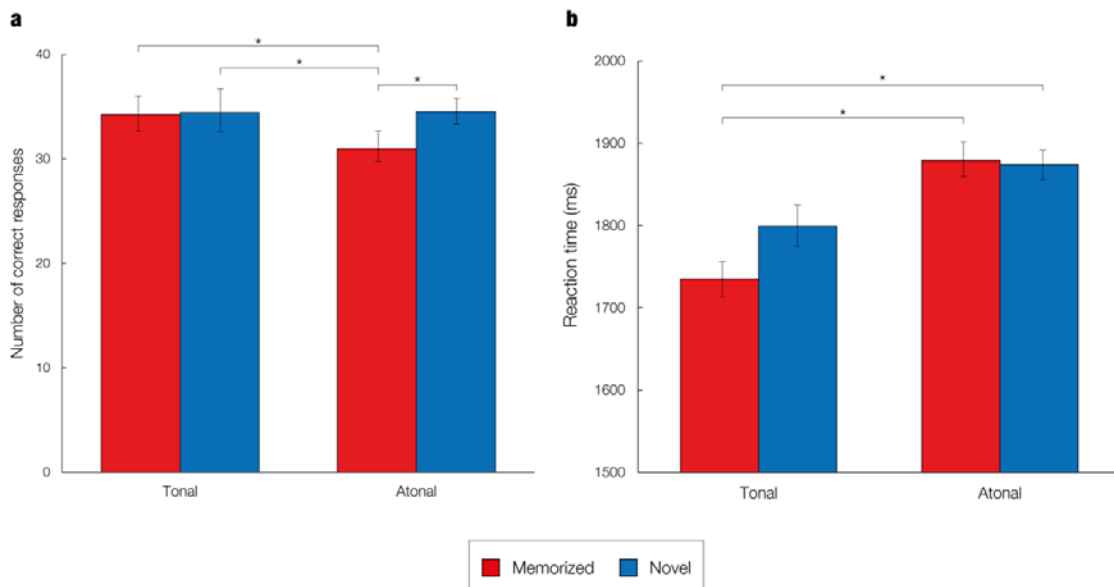
109 **Behavioral data**

110 Participants performed an old/new auditory recognition task. They first listened to a full  
111 musical piece (encoding) and subsequently identified which musical sequences were  
112 memorized or novel. During recognition, the response accuracy and reaction time of the  
113 participants were recorded using a joystick. These behavioral data were statistically analyzed  
114 to examine the differences between the four experimental conditions (memorized tonal  
115 sequences, novel tonal sequences, memorized atonal sequences, novel atonal sequences).

116 A one-way analysis of variance (ANOVA) showed that the differences in response  
117 accuracy were statistically significant,  $F(3, 280) = 6.87, p = .002$ . Post-hoc analyses indicated  
118 that the average number of correct responses was significantly lower for memorized atonal  
119 sequences ( $M = 30.98, SD = 5.46$ ) than for novel atonal ( $M = 34.51, SD = 4.26, p < .001$ ),  
120 memorized tonal ( $M = 34.34, SD = 5.95, p = .002$ ) and novel tonal sequences ( $M = 34.41, SD$   
121  $= 6.04, p = .001$ ). **Figure 2A** shows the average number of correct responses, standard  
122 deviation, and statistically significant differences per condition.

123 Regarding the mean reaction time, there was a statistically significant difference between  
124 conditions as determined by one-way ANOVA,  $F(3, 280) = 4.94, p = .002$ . Post-hoc analyses  
125 revealed that the average reaction time was significantly lower for memorized tonal  
126 sequences ( $M = 1735.17, SD = 259.91$ ) compared to memorized atonal ( $M = 1879.44, SD =$   
127  $259.34, p = .005$ ) and novel atonal sequences ( $M = 1873.78, SD = 250.48, p = .007$ ), but not  
128 compared to novel tonal sequences ( $M = 1799.52, SD = 267.14, p = .450$ ). **Figure 2B**  
129 displays the mean reaction time, standard deviation, and statistically significant differences  
130 per condition.

131



132

133 **Figure 2. Analyses of behavioral data**

134 a – Average number of correct responses for each of the experimental conditions. Asterisks denote a statistically  
135 significant difference between two conditions. Error bars show the standard deviation. b – Average reaction  
136 times for each of the experimental conditions. Asterisks denote a statistically significant difference between two  
137 conditions. Error bars show the standard deviation.

138

139 **MEG sensor data**

140 The MEG data (204 planar gradiometers and 102 magnetometers) were analyzed at the MEG  
141 sensor level, using the broadband signal. Although the emphasis of the study lays in  
142 identifying the brain areas involved in recognizing tonal versus atonal musical sequences, the  
143 MEG sensor data were examined to assess whether the neural signal was significantly  
144 different for memorized than for novel trials and thus would corroborate the results  
145 of previous studies<sup>17, 19</sup>.

146 After averaging the epoched data of correct trials for each experimental condition and  
147 combining the planar gradiometers, paired-samples t-tests were performed to identify which  
148 condition (memorized or novel) generated a stronger neural signal for each time sample and  
149 MEG sensor. Cluster-based MCS were then calculated to correct for multiple comparisons.  
150 This was performed independently for both tonal and atonal data (see Methods for details).

151 First, paired-samples t-tests ( $\alpha = .01$ ) were calculated for the tonal data in the time  
152 interval 0 – 2500 ms (from the onset of the trial) using combined planar gradiometers as these  
153 sensors are less affected by external noise than magnetometers<sup>42-45</sup>. Next, multiple  
154 comparisons were corrected by using cluster-based MCS on the significant t-tests' results ( $\alpha$   
155 = .001, 1000 permutations). Three main significant clusters of activity were identified in

156 three specific time intervals when contrasting memorized versus novel sequences, as reported  
157 in **Table 1** and in Supplementary Materials (**Figure SF1** and **Table ST1**). Additionally, two  
158 main significant clusters of activity were detected when contrasting novel versus memorized  
159 sequences (**Table 1**, **Figure SF2**, and **Table ST1**).

160

Cluster number	Size	MEG channels	Time interval (seconds)	p-value
<i>Memorized versus novel tonal sequences</i>				
1	224	63	0.14 – 0.187	<.001
2	180	29	0.987 – 1.153	<.001
3	150	37	0.807 – 0.887	<.001
<i>Novel versus memorized tonal sequences</i>				
1	277	36	0.64 – 0.8	<.001
2	242	30	0.38 – 0.513	<.001

161

162 **Table 1**

163 Significant clusters of activity for the tonal MEG sensor data.

164

165 Regarding the atonal data, paired-samples t-tests ( $\alpha = .01$ ) were calculated in the same  
166 time interval (0 – 2500 ms) using combined planar gradiometers. Next, multiple comparisons  
167 were corrected for by using MCS on the significant t-tests' results ( $\alpha = .001$ , 1000  
168 permutations). This procedure identified three main significant clusters of activation when  
169 contrasting memorized versus novel excerpts (**Table 2**, **Figure SF3**, and **Table ST1**). In the  
170 case of the novel versus memorized contrast, three main significant clusters of activity were  
171 found (**Table 2**, **Figure SF4**, and **Table ST1**).

172

Cluster number	Size	Channels	Time interval (seconds)	p-value
<i>Memorized versus novel atonal sequences</i>				
1	288	40	0.68 – 0.9	<.001
2	215	44	0.52 – 0.66	<.001
3	135	40	0.133 – 0.187	<.001
<i>Novel versus memorized atonal sequences</i>				
1	478	52	1.167 – 1.267	<.001
2	345	42	0.893 – 0.987	<.001
3	320	44	0.653 – 0.74	<.001

173

174 **Table 2**

175 Significant clusters of activity for the tonal MEG sensor data.

176

177 **Source reconstruction**

178 After examining the strength of the neural signals at the MEG sensor level, we focused on the  
179 main aim of the study, namely to investigate the neural differences underlying the recognition  
180 of tonal versus atonal musical sequences in MEG reconstructed source space. To perform this  
181 analysis, we localized the brain sources of the neural signal recorded by the MEG channels.  
182 This was performed for both the tonal and atonal data and for two frequency bands (delta [0.1  
183 – 1 Hz] and theta [2 – 8 Hz]) that were previously described by Bonetti et al.<sup>38, 40</sup> and  
184 presumably linked to the processing of the single components (theta) relative to the wholistic  
185 sequence (delta).

186

187 *Delta band (0.1 – 1 Hz)*

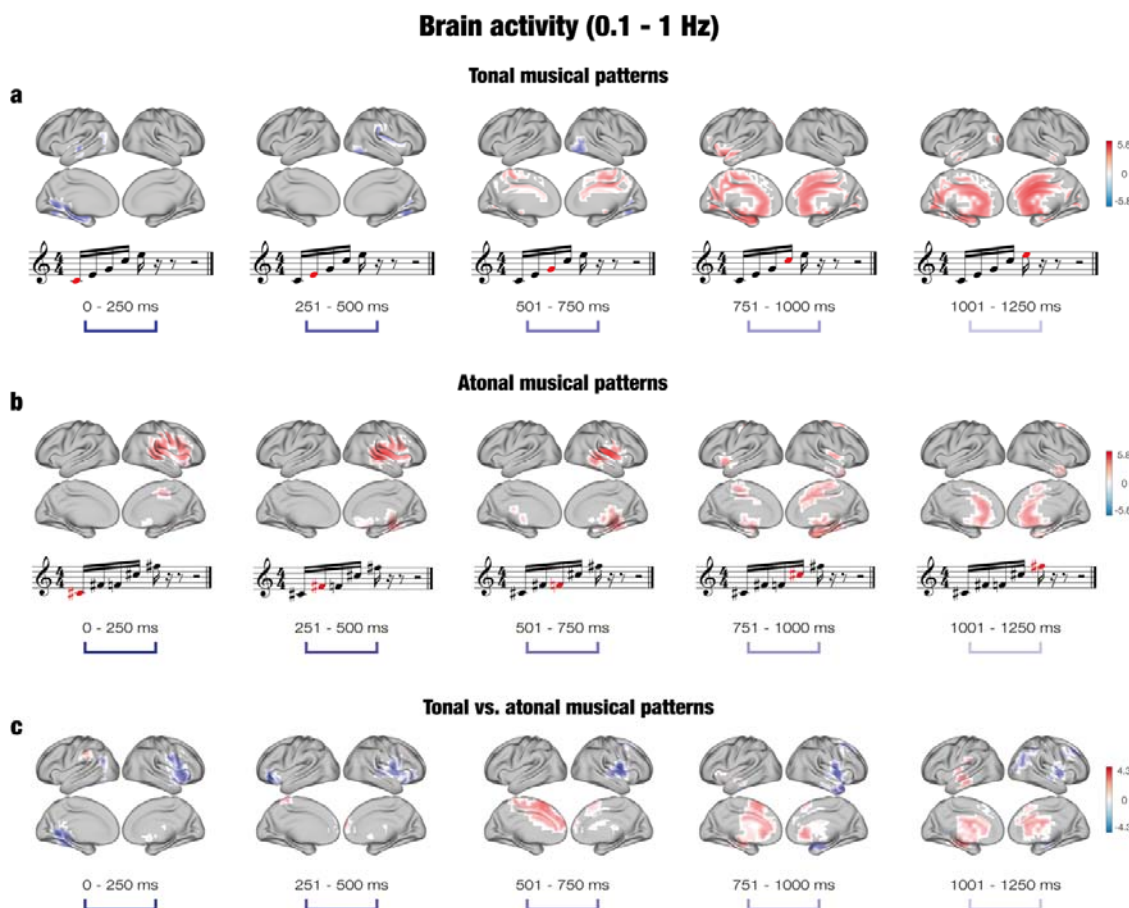
188 The neural sources were calculated using a beamformer approach. First, a forward model was  
189 computed by considering each brain source as an active dipole and calculating its strength  
190 across the MEG sensors. Second, a beamforming algorithm was used as an inverse model to  
191 estimate the brain sources of the neural activity based on the MEG recordings.

192 After computing the neural sources, a GLM was calculated at each timepoint and dipole  
193 location. A series of t-tests ( $\alpha = .05$ ) was carried out at the first and group level to estimate  
194 the main effect of memorized and novel conditions and their contrast for both the tonal and  
195 atonal data independently. Cluster-based MCS ( $\alpha = .001$ , 1000 permutations) were computed  
196 to correct for multiple comparisons and to determine the brain activity underlying the  
197 development of the musical sequences. These analyses were carried out for five specific time  
198 intervals that corresponded to each of the tones comprising the sequences: first tone (0 – 250  
199 ms), second tone (251 – 500 ms), third tone (501 – 750 ms), fourth tone (751 – 1000 ms), and  
200 fifth tone (1001 – 1250 ms). This was estimated for the memorized versus novel contrast for  
201 both tonal and atonal sequences independently and for memorized tonal versus memorized  
202 atonal sequences.

203 Significant clusters of activity ( $p < .001$ ) were located across a number of brain voxels  
204 ( $k$ ) for each tone of the tonal sequences, as reported in **Table ST2**. For memorized tonal  
205 sequences, the neural activity was overall stronger for the third ( $k = 69$ ), fourth ( $k = 266$ ), and  
206 fifth tones ( $k = 229$ ). The largest differences were localized in the middle cingulate gyrus,

207 right supplementary motor area, precuneus, and left lingual gyrus for the third tone; the left  
208 amygdala, left parahippocampal gyrus, left lingual gyrus, left hippocampus, and middle  
209 cingulate gyrus for the fourth tone, and the anterior and middle cingulate gyrus and left  
210 lingual gyrus for the last tone. For novel tonal sequences, the brain activity was stronger  
211 for the first ( $k = 54$ ) and second tones ( $k = 29$ ). In particular, the difference between novel  
212 and memorized sequences was strongest in the left calcarine fissure, left lingual gyrus, left  
213 hippocampus, left precuneus, and left superior temporal gyrus for the first tone, and the right  
214 fusiform gyrus, right lingual gyrus, and right inferior occipital gyrus for the second tone. The  
215 contrast between memorized and novel tonal sequences for the delta band is depicted in  
216 **Figure 3A**.

217  
218



219  
220

221 **Figure 3. Brain activity underlying the recognition of musical sequences at the delta band (0.1 - 1**  
222 **Hz)**

223 **a** – For tonal sequences, the brain activity was stronger for memorized than novel sequences, particularly for the  
224 third (501 – 750 ms), fourth (751 – 1000 ms), and fifth (1001 – 1250) tones. The difference was localized in  
225 memory processing areas such as the cingulate gyrus, hippocampus, and parahippocampal gyrus. **b** – For atonal  
226 sequences, the brain activity was stronger for memorized than novel sequences for all tones. The difference was  
227 mainly localized in auditory processing areas (e.g., superior temporal gyrus, Heschl's gyrus) for the first three  
228 tones, and in memory processing areas (e.g., parahippocampal gyrus, hippocampus) for the fourth and fifth  
229 tones. **c** – For the contrast between tonal and atonal sequences, the brain activity was localized in memory  
230 processing areas for tonal sequences, particularly for the last three tones, and in auditory processing areas for  
231 atonal sequences for all tones.

232

233 In the case of atonal sequences, significant clusters of activity were located for  
234 memorized sequences primarily in the right hemisphere, and the neural activity was stronger  
235 for memorized than novel sequences across all five tones ( $k_1 = 132$ ,  $k_2 = 163$ ,  $k_3 = 130$ ,  $k_4 =$   
236  $140$ ,  $k_5 = 64$ ), as reported in **Table ST2**. In particular, the brain activity was strongest in the  
237 right Rolandic operculum, right superior temporal gyrus, right Heschl's gyrus, right  
238 supramarginal gyrus, and right insula for the first tone; the right Heschl's gyrus, right  
239 superior temporal gyrus, right Rolandic operculum, right middle temporal gyrus, and right  
240 insula for the second tone; the right putamen, right insula, right Rolandic operculum, right  
241 Heschl's gyrus, and right thalamus for the third tone; the parahippocampal gyrus, right  
242 fusiform gyrus, right hippocampus, and putamen for the fourth tone; and the anterior  
243 cingulate cortex, middle frontal gyrus, and caudate nucleus for the last tone. No significant  
244 clusters of activity were located in the delta band for novel atonal sequences. **Figure 3B**  
245 pictures the contrast between memorized and novel atonal sequences in the delta band.

246 Regarding the contrast between memorized tonal and atonal sequences, significant  
247 clusters of activity were located for both types of musical sequences across all tones (see  
248 **Table ST2**). For tonal sequences, the number of significant voxels was higher for the third ( $k$   
249 = 70) and fifth tones ( $k = 79$ ), whereas for atonal sequences the number of significant brain  
250 voxels was higher for the first ( $k = 98$ ), second ( $k = 80$ ), and fourth tones ( $k = 103$ ). In the  
251 case of memorized tonal sequences, the neural activity was localized in the the supplementary  
252 motor area, left median cingulate gyrus, and superior frontal gyrus for the third tone, and the  
253 left hippocampus, left superior temporal gyrus, left thalamus, left insula, left putamen, and  
254 left parahippocampal gyrus for the fifth tone. For memorized atonal sequences, the neural  
255 activity was localized in the left lingual gyrus, left precuneus, left calcarine fissure, middle  
256 temporal gyrus, and right insula at the first tone; the inferior frontal gyrus, right precentral  
257 gyrus, right Rolandic operculum, and right superior temporal gyrus for the second tone; the

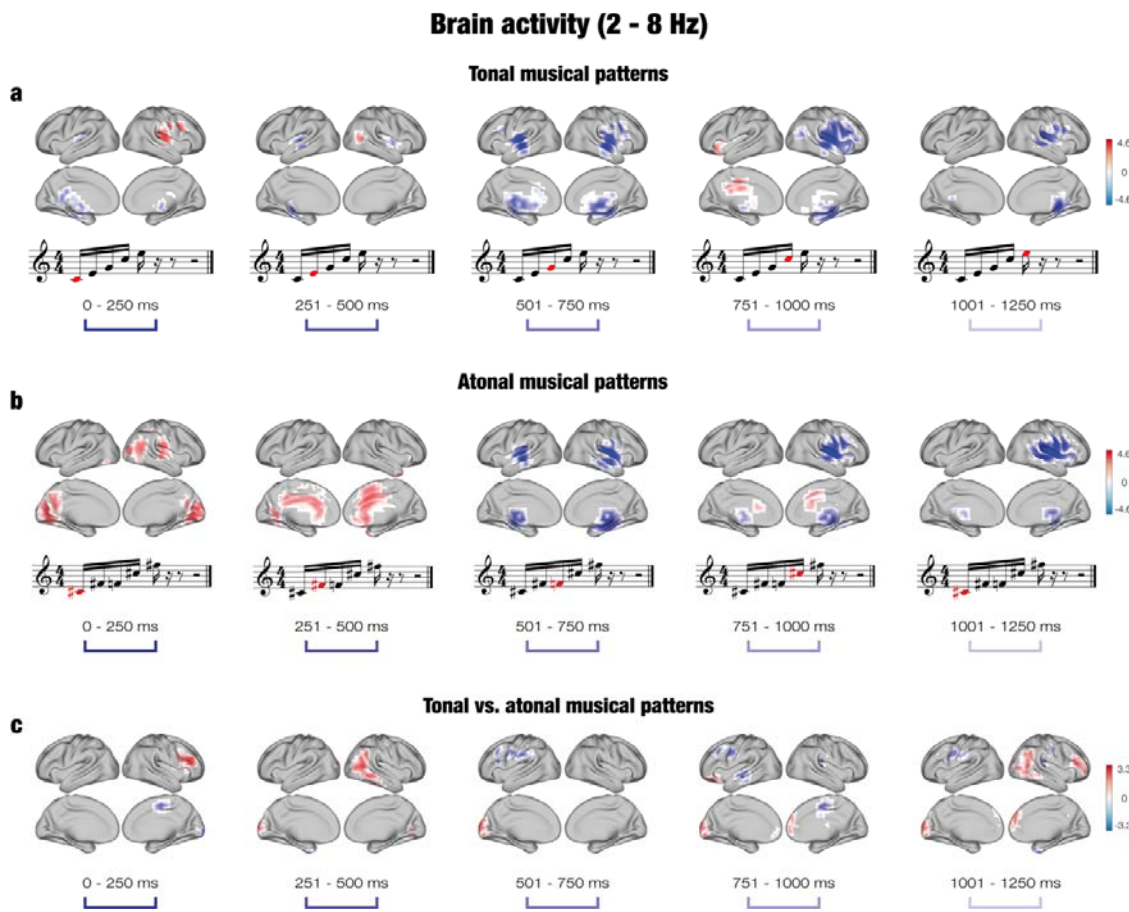
258 right Rolandic operculum, right middle frontal gyrus, right postcentral gyrus, right putamen,  
259 and right insula for the fourth tone; and the right middle frontal gyrus, right angular gyrus,  
260 and right thalamus for the last tone. The contrast between memorized tonal and atonal  
261 sequences in the delta band is shown in **Figure 3C**.

262

263 *Theta band (2 – 8 Hz)*

264 The same procedure was carried out for assessing the brain activity underlying the  
265 recognition of musical sequences in the fast frequency band (2 – 8 Hz). Once the GLM was  
266 computed, cluster-based MCS ( $\alpha = .001$ , 1000 permutations) were calculated for five time  
267 intervals corresponding to each of the five tones that formed the sequence. Again, this was  
268 estimated for the memorized versus novel contrast for both tonal and atonal sequences  
269 and memorized tonal versus memorized atonal sequences.

270 Regarding the contrast for tonal sequences, significant clusters of activity ( $p < .001$ )  
271 were located in multiple brain voxels for both memorized and novel sequences, as reported in  
272 **Table ST2**. For memorized tonal sequences, the neural activity was overall stronger for the  
273 first tone ( $k = 74$ ), whereas it was stronger for novel tonal sequences for the second ( $k = 36$ ),  
274 third ( $k = 200$ ), fourth ( $k = 196$ ), and fifth tones ( $k = 70$ ). The brain activity was localized in  
275 the right Rolandic operculum, right insula, right Heschl's gyrus, and right superior temporal  
276 gyrus for the first tone for memorized tonal sequences. For novel tonal sequences, the main  
277 active areas were the left superior temporal gyrus, insula, Heschl's gyrus, and left  
278 hippocampus for the second tone; Heschl's gyrus, superior temporal gyrus, insula, and  
279 putamen ( $k = 11$ ) for the third tone; right Heschl's gyrus, right insula, right Rolandic  
280 operculum, and right superior temporal gyrus for the fourth tone; and the right Rolandic  
281 operculum, right Heschl's gyrus, right hippocampus, and right thalamus for the fifth tone.  
282 **Figure 4A** displays the contrast between memorized and novel tonal sequences.



302 for memorized sequences, and for the third ( $k = 189$ ), fourth ( $k = 118$ ), and fifth tones ( $k =$   
303 156) for novel sequences, as reported in **Table ST2**. For memorized atonal sequences, the  
304 neural activity was strongest at the calcarine fissure, lingual gyrus, and right Rolandic  
305 operculum for the first tone, and the cingulate gyrus, right supplementary motor area, and  
306 superior frontal gyrus for the second tone. For novel atonal sequences, the neural activity was  
307 strongest at the insula, putamen, superior temporal gyrus, and Heschl's gyrus for the third  
308 tone; the right insula, right putamen, right Heschl's gyrus, right Rolandic operculum, and  
309 right superior temporal gyrus for the fourth tone; and the right insula, right Rolandic  
310 operculum, right Heschl's gyrus, right putamen, and right superior temporal gyrus for the  
311 fifth tone. The contrast between memorized and novel atonal sequences for the theta band is  
312 shown in **Figure 4B**.

313 Finally, the significant clusters of activity in the tonal versus atonal contrast for the theta  
314 band are reported in **Table ST2**. In the case of memorized tonal sequences, the number of  
315 significant brain voxels was higher for the first ( $k = 20$ ), second ( $k = 44$ ), fourth ( $k = 45$ ), and  
316 fifth tones ( $k = 71$ ). The neural activity was located in the right inferior frontal gyrus and right  
317 middle frontal gyrus for the first tone; the right middle temporal gyrus, right inferior parietal  
318 gyrus, right angular gyrus, middle occipital gyrus, and left superior occipital gyrus for the  
319 second tone; the frontal gyrus for the fourth tone; and the right middle occipital gyrus, right  
320 frontal gyrus, and right middle temporal gyrus for the fifth tone. For memorized atonal  
321 sequences, the number of significant voxels was higher for the third tone ( $k = 38$ ) and the  
322 neural activity was mainly localized in the left inferior frontal gyrus, left middle frontal  
323 gyrus, left supramarginal gyrus, and right supplementary motor area. **Figure 4C** shows the  
324 contrast between tonal and atonal sequences for the theta band.

325 Altogether, we found significant differences between tonal and atonal sequences,  
326 especially for the slow frequency band. Recognition of memorized tonal sequences elicited  
327 stronger neural activity in left cingulate and hippocampal areas in the last three tones of the  
328 sequences, whereas recognition of memorized atonal sequences was supported by activation  
329 in right auditory regions from the second tone onwards.

330 **Discussion**

331 This study set out to investigate the brain activation underlying the recognition of auditory  
332 musical sequences characterized by different levels of complexity (tonal and atonal).  
333 Behavioral data showed clear differences between the recognition of tonal and atonal  
334 sequences and significant clusters of activation were observed at the MEG sensor level.  
335 Source reconstruction analyses indicated different activation clusters for tonal and atonal  
336 sequences, particularly in the delta frequency band. Overall, the neural activity was stronger  
337 in memory processing areas for memorized tonal sequences and in auditory processing  
338 regions for memorized atonal sequences.

339 Prior to focusing on the differences in brain activity related to distinct levels of  
340 recognition complexity, we verified that the current results were consistent with previous  
341 studies. Indeed, the brain areas activated during the recognition of tonal sequences confirmed  
342 the involvement of a widespread brain network including both auditory and memory  
343 processing regions <sup>36-38, 40</sup>. Furthermore, in accordance with previous research, the neural  
344 activity was clearly distributed in two frequency bands <sup>38, 39</sup>. Delta band (0.1 – 1 Hz) was  
345 linked to the recognition of the whole auditory sequences (*global processing*), which was  
346 reflected by the stronger activation occurring in this band for the recognition of the  
347 memorized sequences. Conversely, theta band (2 – 8 Hz) was associated with the processing  
348 of the individual tones (*local processing*), as suggested by the stronger neural activity in  
349 auditory regions during processing of novel sequences.

350 Regarding the recognition of tonal and atonal sequences, we observed distinct neural  
351 pathways when processing and recognizing the two types of auditory stimuli. While the  
352 recognition of tonal sequences mainly recruited a widespread brain network involving  
353 cingulate gyrus and hippocampus in the right hemisphere, the recognition of atonal sequences  
354 was mainly associated with a sustained, slow activity in the left auditory cortex. These results  
355 can be interpreted in light of different theoretical frameworks, namely predictive coding,  
356 harmonicity, and global neuronal workspace (GNW). According to PCM theory, the brain's  
357 predictive model is being continuously updated while listening to music in order to decrease  
358 precision-weighted prediction errors <sup>16, 18, 19</sup>. The predictive value of atonal music is weaker  
359 than tonal music, which alters its complexity and increases prediction errors <sup>42-46, 49</sup>. In turn,  
360 this change in stimulus predictability undermines the processing <sup>42-46</sup> and enjoyment <sup>46-48</sup> of  
361 atonal music. This was apparent when examining the behavioral results, since memorized  
362 atonal sequences were more slowly and less accurately recognized. In addition, the

363 distribution of the neural activity in two frequency bands suggests a combination of top-down  
364 predictions in the delta band, which is related to the recognition of memorized sequences, and  
365 bottom-up predictions in the theta band, as the prediction error increases with novel  
366 sequences.

367 An alternative explanation for these results focuses on the harmonicity of auditory  
368 stimuli. Tonal music has been closely linked to the harmonic series, a natural sequence of  
369 sound frequencies that are integer multiples of a fundamental. Environmental sounds are  
370 typically nonharmonic, whereas both human and animal vocalizations contain harmonic  
371 structures<sup>63</sup>. The tonotopic organization of the human auditory cortex is particularly sensitive  
372 to harmonic tones, suggesting that this region developed to process harmonics due to their  
373 relevance for social communication<sup>64, 65</sup>. These results indicate that distinct neural pathways  
374 are activated when recognizing auditory stimuli that are not coherent with the natural  
375 harmonic series and thus arguably more complex to process. Indeed, we found that for  
376 memorized tonal sequences, the brain activity was primarily located at the cortico-  
377 hippocampal network in the right hemisphere, and for memorized atonal sequences the  
378 auditory network in the left hemisphere. Specifically, the strong activation in low-processing  
379 primary auditory regions at the first three tones of the atonal sequences suggests a  
380 “disentangling” of the sequence before it can be processed and recognized by high-cognitive  
381 areas involved in memory processing. One possible approach to further test the harmonicity  
382 hypothesis in relation to sequence recognition would be to create a collection of pieces that  
383 are systematically varied in terms of their similarity to the natural harmonic series. Future  
384 studies are called to investigate such perspectives.

385 Finally, the current results are also consistent with the GNW hypothesis<sup>66, 67</sup>. According  
386 to this theory, stimuli become conscious when they ignite late, high-order regions in response  
387 to the activation of sensory cortices involved in perceptual representation. Conversely,  
388 unconscious information does not reach high-processing brain areas and neural activity is  
389 limited to sensory cortices<sup>66, 68, 69</sup>. Importantly, we found that tonal sequences induced a late  
390 and robust activation of memory processing regions. Although it is unclear *why* atonal  
391 sequences were differently processed by the brain, we can confirm that the complexity of the  
392 stimuli modulates the transition from primary sensory areas to the GNW, adding new  
393 information to this comprehensive theoretical framework.

394 The current study provides valuable insights into the brain mechanisms underlying the  
395 recognition of auditory sequences. The results are consistent with those of previous studies  
396 and evidence of the engagement of a large brain network that comprises both memory

397 processing and auditory regions when recognizing music. Results further highlight the  
398 importance of stimulus complexity for the processing of temporal sequences and hint that the  
399 brain employs different strategies to account for this complexity.

400 **Acknowledgements**

401 We thank Giulia Donati, Riccardo Proietti, Giulio Carraturo, Mick Holt, Holger Friis for  
402 their assistance in the neuroscientific experiment.

403 The Center for Music in the Brain (MIB) is funded by the Danish National Research  
404 Foundation (project number DNRF117). Additionally, we thank the Fundación Mutua  
405 Madrileña for the economic support provided to the author GFR and the University of  
406 Bologna for the economic support provided to student assistants Giulia Donati, Riccardo  
407 Proietti and Giulio Carraturo.

408 LB is supported by Carlsberg Foundation (CF20-0239), Center for Music in the Brain,  
409 Linacre College of the University of Oxford, and Society for Education and Music  
410 Psychology (SEMPRE's 50th Anniversary Awards Scheme).

411 MLK is supported by Center for Music in the Brain and Centre for Eudaimonia and  
412 Human Flourishing, which is funded by the Pettit and Carlsberg Foundations.

413 **Author contributions**

414 LB, EB, MLK, and PV conceived the hypotheses, designed the study, and recruited the  
415 resources for the experiment. LB and GFR performed pre-processing and statistical  
416 analysis. EB, SAK, LB, MLK, and PV provided essential help to interpret and frame the  
417 results within the neuroscientific literature. GFR and LB wrote the first draft of the  
418 manuscript and prepared the figures. All the authors contributed to and approved the final  
419 version of the manuscript.

420 **Competing interests' statement**

421 The authors declare no competing interests.

422 **Materials and methods**

423 **Participants**

424 The participant sample consisted of 71 volunteers (38 males and 33 females) aged 18 to 42  
425 years old (mean age:  $25 \pm 4.10$  years). All participants were healthy and reported normal  
426 hearing. Participants were recruited in Denmark and came from Western countries with  
427 matching socioeconomic and educational backgrounds.

428 The project was approved by the Ethics Committee of the Central Denmark Region (De  
429 Videnskabsetiske Komitéer for Region Midtjylland, Ref 1-10-72-411-17). The experimental  
430 procedures were carried out in compliance with the Declaration of Helsinki – Ethical  
431 Principles for Medical Research. All participants gave the informed consent before starting  
432 the experimental procedure.

433

434 **Experimental stimuli and design**

435 Two musical compositions were used in the experiment: the right-hand part of Johann  
436 Sebastian Bach's Prelude No. 1 in C Major, BWV 846 (hereafter referred to as the “tonal  
437 piece”), and an atonal version of the prelude (hereafter referred to as the “atonal piece”).  
438 MIDI versions were created using Finale (MakeMusic, Boulder, CO) and both pieces lasted  
439 2.5 minutes each, with the same duration for all tones. LB composed the atonal piece based  
440 on the tonal piece. In particular, new tones were assigned to each of the tones comprising  
441 Bach's original prelude. These new tones were one or two semitones higher or lower than the  
442 original tones, and the same tone conversion was applied throughout the entire tonal piece to  
443 obtain the atonal piece (e.g., every C tone in the tonal piece was converted into a C sharp in  
444 the atonal piece). Thus, both compositions were identical in terms of the sequential  
445 presentation of the tones (i.e., if C was positioned as 1<sup>st</sup>, 7<sup>th</sup>, and 8<sup>th</sup> tone in the tonal piece, C  
446 sharp occupied the same positions [1<sup>st</sup>, 7<sup>th</sup>, and 8<sup>th</sup>] in the atonal piece), their rhythmic  
447 pattern, dynamics, and duration. Thus, the crucial difference between the two pieces was that  
448 the tonal piece was in the key of C Major, whereas the atonal piece did not have a musical  
449 key. The first two bars of each piece are displayed in **Figure 1a**, showing similarities and  
450 correspondence between the two pieces.

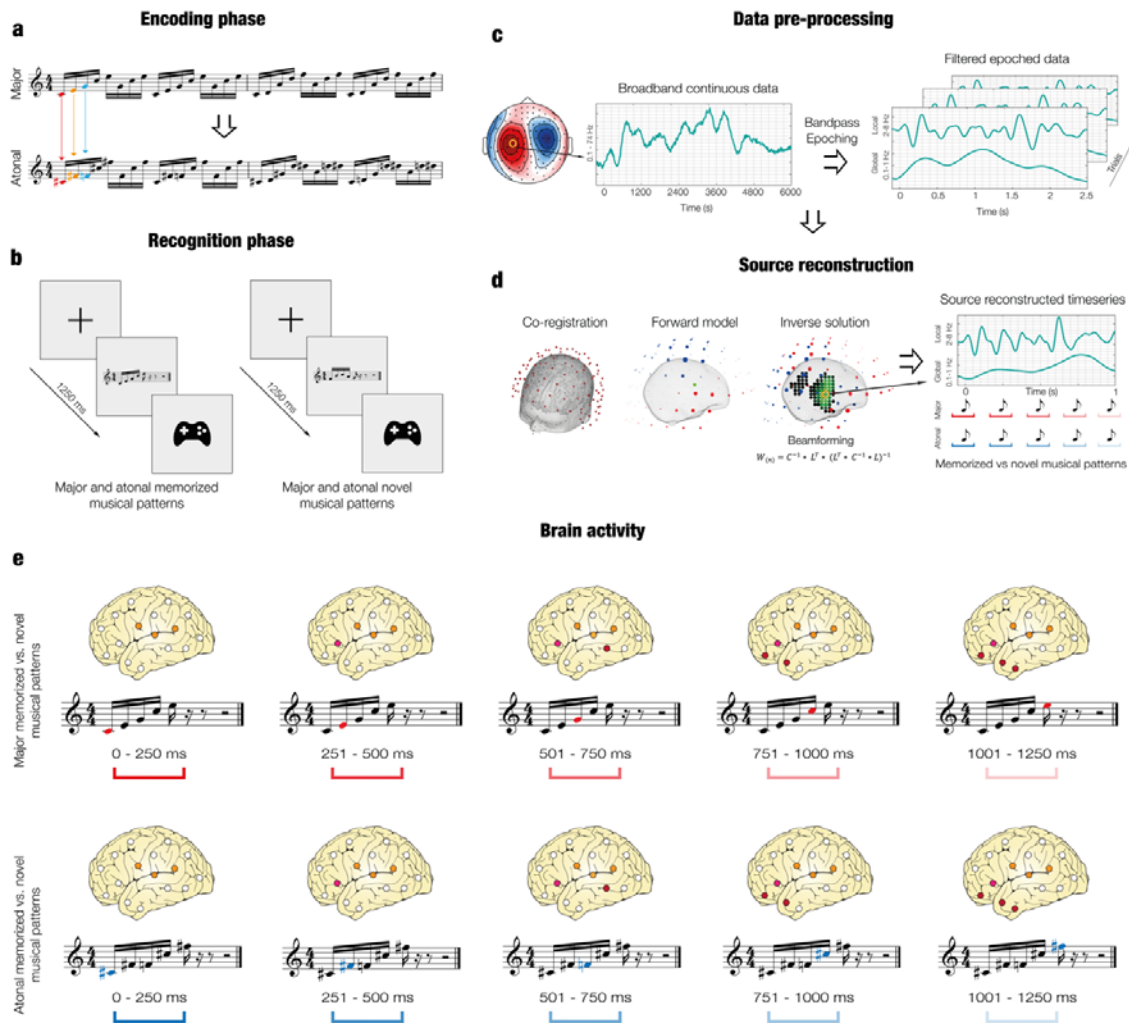
451 Forty musical excerpts (i.e., short melodies or sequences) were extracted from each of  
452 the pieces. All excerpts consisted of the first five notes of each bar and lasted for 1250 ms  
453 (250 ms per note). In addition, 40 new excerpts were created for each piece based on the  
454 original ones. These new sequences were matched to the original ones among several

455 variables, to prevent potential confounds. Specifically, they were matched for rhythm,  
456 volume, timbre, tempo, meter, and tonality.

457 The stimuli were employed in an old/new auditory recognition paradigm, as depicted in  
458 **Figure 1b**, that was administered to the participants while their brain activity was recorded  
459 using MEG. The paradigm consisted of two parts, encoding and recognition, and was  
460 performed twice, once for the tonal piece and once for the atonal piece. The order of  
461 tonal/atonal was counterbalanced across participants. During the encoding part, participants  
462 actively listened to four repetitions of the entire musical piece (tonal or atonal) and tried to  
463 memorize it as much as possible. Afterwards, they were presented with the previously  
464 described 80 musical excerpts (40 memorized and 40 novel excerpts, randomly ordered) and  
465 stated whether the excerpts belonged to the piece they had previously listened to  
466 (“memorized”) or whether they were new excerpts (“novel”). Response accuracy and reaction  
467 time were recorded using a joystick.

468

469



470

471

472 **Figure 1. Experimental stimuli and design, data analyses and (temporal) brain activity**

473 **a** – Two musical pieces were used in the experiment: the right-hand part of J. S. Bach’s Prelude No. 1 in C  
 474 Major, BWV 846 (i.e., “tonal”, top row), and an atonal version of the prelude (i.e., “atonal”, bottom row). Both  
 475 pieces were matched in terms of the sequential presentation of the tones, rhythmic patterns, dynamics, and  
 476 duration, and their melodic contour was almost identical. The atonal piece was created by LB by assigning new  
 477 tones that were one or two semitones lower or higher than the original tones of the tonal piece. For example, C  
 478 (in red) was converted into C sharp (in red), E (in orange) was converted into F sharp (in orange), G (in blue)  
 479 was converted into F (in blue), etc. **b** – Participants performed the experimental task twice (once for the tonal  
 480 piece and once for the atonal piece) and the order of presentation was randomized across participants. After  
 481 listening to the full piece, participants were presented with excerpts that belonged to the piece or with new  
 482 excerpts and were asked to state whether the excerpts were “memorized” or “novel” using a joystick. **c** – The  
 483 task was administered to the participants while their brain activity was recorded using MEG. The continuous  
 484 neural data was preprocessed. **d** – Source reconstruction analyses were conducted to identify the brain sources  
 485 that generated the neural activity. The data was first bandpass-filtered into two frequency bands (0.1 – 1 Hz and  
 486 2 – 8 Hz) and the MEG and MRI data were co-registered. An overlapping-spheres forward model was computed

487 using an 8-mm grid and a beamforming algorithm was applied as the inverse solution. Finally, the source  
488 reconstructed time series was computed for both tonal and atonal data and their contrast in both frequency  
489 bands. **e** – Contrasts between memorized and novel sequences were calculated for each tone that comprised the  
490 tonal and atonal musical sequences for both frequency bands.

491

## 492 **Data acquisition**

493 The MEG recordings were acquired in a magnetically shielded room at Aarhus University  
494 Hospital (Denmark) with an Elekta Neuromag TRIUX MEG scanner with 306 channels  
495 (Elekta Neuromag, Helsinki, Finland). The data were recorded at a sampling rate of 1000 Hz  
496 with an analogue filtering of 0.1 – 330 Hz. Before starting the recordings, the head shape of  
497 the participants and the position of four Head Position Indicator (HPI) coils with respect to  
498 three anatomical landmarks were registered using a 3D digitizer (Polhemus Fastrak,  
499 Colchester, VT, USA). This information was later used to co-register the MEG data with the  
500 MRI anatomical scans. During the MEG recordings, the HPI coils registered the continuous  
501 head localization, which was subsequently used for movement correction analyses.  
502 Additionally, two sets of bipolar electrodes were used to record eye movements and cardiac  
503 rhythm for later removing electrooculography (EOG) and electrocardiography (ECG)  
504 artifacts.

505 The MRI scans were recorded on a CE-approved 3T Siemens MRI-scanner at Aarhus  
506 University Hospital (Denmark). The data were recorded using a structural T1 with a spatial  
507 resolution of 1.0 x 1.0 x 1.0 mm and the following sequence parameters: echo time (TE) =  
508 2.96 ms, repetition time (TR) = 5000 ms, reconstructed matrix size = 256 x 256, bandwidth =  
509 240 Hz/Px.

510 The MEG and MRI recordings were acquired in two separate sessions.

511

## 512 **Data preprocessing**

513 The raw MEG sensor data (204 planar gradiometers and 102 magnetometers) were first  
514 preprocessed by MaxFilter<sup>50</sup> in order to suppress external interferences. In addition, the data  
515 were corrected for head motion and downsampled to 250 Hz. The data were then converted  
516 into Statistical Parametric Mapping (SPM)<sup>51</sup> format and analyzed in MATLAB (MathWorks,  
517 Natick, MA, USA) with the Oxford Centre for Human Brain Activity (OHBA) Software  
518 Library (OSL) (<https://ohba-analysis.github.io/osl-docs/>), a freely available software that  
519 builds upon Fieldtrip<sup>52</sup>, FSL<sup>53</sup>, and SPM toolboxes. The signal was high-pass filtered (0.1  
520 Hz of cutoff) to remove external frequencies and a notch filter was subsequently applied (48

521 – 52 Hz) to correct for inferences of the electric current. The signal was further downsampled  
522 to 150 Hz and the continuous MEG data were visually inspected to remove artifacts using the  
523 OSLview tool. An independent component analysis (ICA) was performed to remove EOG  
524 and ECG components. After reconstructing the signal with the remaining components<sup>54</sup>, the  
525 data were epoched into 160 trials (80 excerpts from each musical piece). Each trial lasted  
526 1350 ms (1250 ms plus 100 ms of baseline time) and further analyses were performed on  
527 correctly identified trials only (see **Figure 1C**).

528 The raw MEG sensor data (204 planar gradiometers and 102 magnetometers) were first  
529 preprocessed by MaxFilter<sup>50</sup> in order to suppress external interferences. In addition, the data  
530 were corrected for head motion and downsampled to 250 Hz. The data were then converted  
531 into Statistical Parametric Mapping (SPM)<sup>51</sup> format and analyzed in MATLAB (MathWorks,  
532 Natick, MA, USA) with the Oxford Centre for Human Brain Activity (OHBA) Software  
533 Library (OSL) (<https://ohba-analysis.github.io/osl-docs/>), a freely available software that  
534 builds upon Fieldtrip<sup>52</sup>, FSL<sup>53</sup>, and SPM toolboxes. The signal was high-pass filtered (0.1  
535 Hz of cutoff) to remove external frequencies and a notch filter was subsequently applied (48  
536 – 52 Hz) to correct for inferences of the electric current. The signal was further downsampled  
537 to 150 Hz and the continuous MEG data were visually inspected to remove artifacts using the  
538 OSLview tool. An independent component analysis (ICA) was performed to remove EOG  
539 and ECG components. After reconstructing the signal with the remaining components<sup>54</sup>, the  
540 data were epoched into 160 trials (80 excerpts from each musical piece). Each trial lasted  
541 1350 ms (1250 ms plus 100 ms of baseline time) and further analyses were performed on  
542 correctly identified trials only (see **Figure 1C**).

543

#### 544 **MEG sensor data analysis**

545 The primary focus of this study was on detecting differences in the brain activity underlying  
546 the recognition of tonal versus atonal musical sequences. However, the data were first  
547 analyzed at the MEG sensor level to verify that the neural signal was stronger for memorized  
548 versus novel musical sequences. This first step was essential to replicate previous findings  
549 obtained using a very similar experimental setting and paradigm and thus assess the quality of  
550 our data<sup>38-40</sup>.

551 Following the preprocessing of the neural data, and in accordance with MEG analysis  
552 guidelines<sup>55</sup>, all trials belonging to one condition were averaged together. This procedure  
553 resulted in four mean trials: one for memorized trials and one for novel trials for each musical  
554 piece (i.e., memorized tonal, novel tonal, memorized atonal, novel atonal). Next, each pair of

555 planar gradiometers was combined by a sum root square. Paired-samples t-tests ( $\alpha = .01$ )  
556 were then calculated to contrast the memorized and novel conditions for both the tonal and  
557 atonal pieces, independently. This was performed for each combined planar gradiometer and  
558 each time-point in the time-range 0 – 2500 ms (from the onset of the first tone of the musical  
559 sequences) in order to determine which condition generated a stronger neural signal. The  
560 analyses were calculated for planar gradiometers, since these sensors are less affected by  
561 external noise and thus highly reliable when computing analyses at the MEG sensor level<sup>55-58</sup>.  
562 Multiple comparisons were corrected using cluster-based Monte Carlo simulations (MCS)  
563 ( $\alpha = .001$ , 1000 permutations) on the significant t-tests' results. Specifically, for each  
564 timepoint, a 2D matrix was generated reproducing the spatial location of the MEG channels  
565 and the results of the t-tests of each MEG channel binarized according to their *p*-values (0s  
566 for not significant tests and 1s for significant tests [i.e.,  $p < .01$ ]). The elements of the  
567 resulting 3D matrix were then submitted to 1000 permutations. For each permutation, we  
568 identified the maximum cluster of permuted 1s, and we built a reference distribution using  
569 the maximum cluster sizes detected for each of the 1000 permutations. Finally, the original  
570 clusters that had a larger size than 99.9% of the maximum cluster sizes of the permuted data  
571 were considered significant.

572

### 573 **Source reconstruction**

574 After examining the strength of the neural signals at the MEG sensor level, we focused on the  
575 main aim of the study, which was to investigate the neural differences underlying the  
576 recognition of tonal versus atonal musical sequences in MEG reconstructed source space. To  
577 perform this analysis, we localized the brain sources of the neural signal recorded in the MEG  
578 channels. This procedure required designing a forward model, computing the inverse  
579 solution (in this case, using a beamforming approach), and identifying the statistically  
580 significant brain sources underlying the recognition of tonal and atonal sequences and their  
581 contrasts over time. **Figure 1D** shows the graphical depiction of the source reconstruction  
582 analyses.

583

### 584 *Beamforming*

585 Before computing the source reconstruction algorithm, the continuous data were band-pass  
586 filtered into two frequency bands: a slow band (delta, 0.1 – 1 Hz) and a fast band (theta, 2 – 8  
587 Hz). These bands were selected based on the findings reported by Bonetti et al.<sup>38-40</sup>, which  
588 suggested that the theta band was responsible for a sensorial elaboration of each object (tone)

589 of the sequence, while the delta band was implicated in the recognition of the holistic  
590 temporal sequence. The filtered data were then epoched and the brain sources that generated  
591 the signal were calculated.

592 First, an overlapping-spheres forward model was computed using an 8-mm grid. This  
593 theoretical head model considers each brain source as an active dipole and describes how the  
594 unitary strength of such a dipole is reflected across the MEG sensors <sup>60</sup>. Using the  
595 information collected with the 3D digitizer, the MEG data and individual T1-weighted  
596 images were co-registered and the forward model was subsequently computed. An MNI152-  
597 T1 template with 8-mm spatial resolution was used in four cases in which the individual  
598 anatomical scans were not available. Second, a beamforming algorithm was employed as the  
599 inverse model. This is one of the most widely used algorithms for estimating the brain  
600 sources from MEG channels' data and consists of utilizing a different set of weights which  
601 are sequentially applied to the source locations (dipoles) for isolating the contribution of each  
602 source to the activity recorded by the MEG channels for each time-point <sup>55, 61, 62</sup>.

603

604 *General Linear Model*

605 After estimating the brain sources of the signal recorded on the MEG channels, a General  
606 Linear Model (GLM) was estimated sequentially for each timepoint at each dipole location.  
607 At the first level, the main effect of memorized and novel conditions, as well as their contrast,  
608 was computed independently for each participant. At the group level, t-tests were carried out  
609 for each dipole location to obtain the main effect of tonal, atonal and their contrast computed  
610 on all aggregated participants. The GLMs were estimated independently for both the tonal  
611 and atonal data and for both frequency bands.

612

613 *Brain activity underlying the development of the musical sequences*

614 To determine the temporal evolution of the brain activity underlying musical sequences'  
615 recognition, cluster-based MCS were estimated for five specific time-windows that  
616 corresponded to each of the five tones comprising the musical sequences. This procedure was  
617 carried out independently for both tonal and atonal data and for both frequency bands. Thus,  
618 ten cluster-based MCS were calculated for each musical piece (five tones x two frequency  
619 bands) on the results of the group-level analysis with an adjusted alpha level of .001 ( $\alpha =$   
620  $0.01/10 = .001$ ). This procedure allowed detecting the spatial clusters of significant brain  
621 sources underlying the recognition of the tonal and atonal musical sequences. For each of the  
622 MCSs, the data were sub-averaged in the time-window of interest (e.g., the time-window for

623 the first tone of the musical sequences) and then submitted to 1000 permutations to build a  
624 reference distribution of the maximum cluster sizes detected in the permuted data. Then,  
625 using the same procedure as with the MEG channels, the original cluster sizes were compared  
626 to the reference distribution and were considered significant if their size was bigger than  
627 99.9% of the maximum cluster sizes of the permuted data.

628 Importantly, further analyses were conducted to assess the differences between tonal and  
629 atonal data when recognizing memorized trials for both the delta and theta frequency bands.  
630 For each participant, a t-test ( $\alpha = 0.01$ ) was computed for each source location and for the  
631 five time-windows corresponding to each musical tone, contrasting the brain activity  
632 underlying the recognition of tonal versus atonal music. Multiple comparisons were corrected  
633 for by using cluster-based MCS, as described above. In this case, ten MCS ( $\alpha = .001$ , 1000  
634 permutations) were calculated on the significant t-test results (five tones x two frequency  
635 ranges).

636

637 **Data availability**

638 The code and anonymized neuroimaging data from the experiment will be made available  
639 upon request. Regarding the data, we will be able to share it when it is completely  
640 anonymized and cannot lead in any way to the original participants identity, according to  
641 Danish regulations. Otherwise, a data sharing agreement must be made.

642 **References**

- 643 1. Gabrieli, J.D. Cognitive neuroscience of human memory. *Annual Review of Psychology*  
644 **49**, 87-115; 10.1146/annurev.psych.49.1.87 (1998).
- 645 2. Daumas, S., Halley, H., Frances, B., & Lassalle, J.M. Encoding, consolidation, and  
646 retrieval of contextual memory: differential involvement of dorsal CA3 and CA1  
647 hippocampal subregions. *Learning and Memory* **12**, 375-82; 10.1101/lm.81905 (2005).
- 648 3. Greicius, M.D., Krasnow, B., Boyett-Anderson, J.M., Eliez, S., Schatzberg, A.F., Reiss,  
649 A.L., & Menon, V. Regional analysis of hippocampal activation during memory  
650 encoding and retrieval: fMRI study. *Hippocampus* **13**, 164-74; 10.1002/hipo.10064  
651 (2003).
- 652 4. Meltzer, J.A., & Constable, R.T. Activation of human hippocampal formation reflects  
653 success in both encoding and cued recall of paired associates. *NeuroImage* **24**, 384-97;  
654 10.1016/j.neuroimage.2004.09.001 (2005).
- 655 5. Bird, C.M. The role of the hippocampus in recognition memory. *Cortex* **93**, 155-165;  
656 10.1016/j.cortex.2017.05.016 (2017).
- 657 6. Eichenbaum, H., Yonelinas, A.P., & Ranganath, C. The medial temporal lobe and  
658 recognition memory. *Annual Review of Neuroscience* **30**, 123-52;  
659 10.1146/annurev.neuro.30.051606.094328 (2007).
- 660 7. Wiltgen, B.J., Brown, R.A., Talton, L.E., & Silva, A.J. New circuits for old memories:  
661 the role of the neocortex in consolidation. *Neuron* **44**, 101-8;  
662 10.1016/j.neuron.2004.09.015 (2004).
- 663 8. van Kesteren, M.T., Fernandez, G., Norris, D.G., & Hermans, E.J. Persistent schema-  
664 dependent hippocampal-neocortical connectivity during memory encoding and  
665 postencoding rest in humans. *Proceedings of the National Academy of Sciences of the*  
666 *United States of America* **107**, 7550-5; 10.1073/pnas.0914892107 (2010).
- 667 9. Mehta, M.R. Cortico-hippocampal interaction during up-down states and memory  
668 consolidation. *Nature Neuroscience* **10**, 13-5; 10.1038/nn0107-13 (2007).
- 669 10. Aggleton, J.P., & Brown, M.W. Interleaving brain systems for episodic and recognition  
670 memory. *Trends in Cognitive Sciences* **10**, 455-63; 10.1016/j.tics.2006.08.003 (2006).
- 671 11. DiCarlo, J.J., Zoccolan, D., & Rust, N.C. How does the brain solve visual object  
672 recognition? *Neuron* **73**, 415-34; 10.1016/j.neuron.2012.01.010 (2012).
- 673 12. Sato, W., & Yoshikawa, S. Recognition memory for faces and scenes. *Journal of*  
674 *General Psychology* **140**, 1-15; 10.1080/00221309.2012.710275 (2013).

- 675 13. Dehaene, S., Meyniel, F., Wacongne, C., Wang, L., & Pallier, C. The Neural  
676 Representation of Sequences: From Transition Probabilities to Algebraic Patterns and  
677 Linguistic Trees. *Neuron* **88**, 2-19; 10.1016/j.neuron.2015.09.019 (2015).
- 678 14. Kang, H., Agus, T.R., & Pressnitzer, D. Auditory memory for random time patterns.  
679 *Journal of the Acoustical Society of America* **142**, 2219; 10.1121/1.5007730 (2017).
- 680 15. Peretz, I., & Zatorre, R.J., *The cognitive neuroscience of music*. 2003: OUP Oxford.
- 681 16. Vuust, P., Ostergaard, L., Pallesen, K.J., Bailey, C., & Roepstorff, A. Predictive coding  
682 of music-brain responses to rhythmic incongruity. *Cortex* **45**, 80-92;  
683 10.1016/j.cortex.2008.05.014 (2009).
- 684 17. Vuust, P., Dietz, M.J., Witek, M., & Kringelbach, M.L. Now you hear it: a predictive  
685 coding model for understanding rhythmic incongruity. *Annals of the New York  
686 Academy of Sciences*, 10.1111/nyas.13622 (2018).
- 687 18. Vuust, P., Heggli, O.A., Friston, K.J., & Kringelbach, M.L. Music in the brain. *Nature  
688 Reviews: Neuroscience*, 10.1038/s41583-022-00578-5 (2022).
- 689 19. Koelsch, S., Vuust, P., & Friston, K. Predictive Processes and the Peculiar Case of  
690 Music. *Trends in Cognitive Sciences* **23**, 63-77; 10.1016/j.tics.2018.10.006 (2019).
- 691 20. Schroger, E., Marzecova, A., & SanMiguel, I. Attention and prediction in human  
692 audition: a lesson from cognitive psychophysiology. *European Journal of Neuroscience*  
693 **41**, 641-64; 10.1111/ejn.12816 (2015).
- 694 21. Rohrmeier, M.A., & Koelsch, S. Predictive information processing in music cognition.  
695 A critical review. *International Journal of Psychophysiology* **83**, 164-75;  
696 10.1016/j.ijpsycho.2011.12.010 (2012).
- 697 22. Quiroga-Martinez, D.R., Hansen, N.C., Hojlund, A., Pearce, M., Brattico, E., & Vuust,  
698 P. Decomposing neural responses to melodic surprise in musicians and non-musicians:  
699 Evidence for a hierarchy of predictions in the auditory system. *NeuroImage* **215**,  
700 116816; 10.1016/j.neuroimage.2020.116816 (2020).
- 701 23. Quiroga-Martinez, D.R., Hansen, N.C., Hojlund, A., Pearce, M.T., Brattico, E., &  
702 Vuust, P. Reduced prediction error responses in high-as compared to low-uncertainty  
703 musical contexts. *Cortex* **120**, 181-200; 10.1016/j.cortex.2019.06.010 (2019).
- 704 24. Lumaca, M., Trusbak Haumann, N., Brattico, E., Grube, M., & Vuust, P. Weighting of  
705 neural prediction error by rhythmic complexity: A predictive coding account using  
706 mismatch negativity. *European Journal of Neuroscience* **49**, 1597-1609;  
707 10.1111/ejn.14329 (2019).

- 708 25. Koelsch, S., Fritz, T., Schulze, K., Alsop, D., & Schlaug, G. Adults and children  
709 processing music: an fMRI study. *NeuroImage* **25**, 1068-76;  
710 10.1016/j.neuroimage.2004.12.050 (2005).
- 711 26. Putkinen, V., Tervaniemi, M., & Huotilainen, M. Musical playschool activities are  
712 linked to faster auditory development during preschool-age: a longitudinal ERP study.  
713 *Scientific Reports* **9**, 11310; 10.1038/s41598-019-47467-z (2019).
- 714 27. Pearce, M.T. Statistical learning and probabilistic prediction in music cognition:  
715 mechanisms of stylistic enculturation. *Annals of the New York Academy of Sciences*,  
716 10.1111/nyas.13654 (2018).
- 717 28. Witek, M.A., Clarke, E.F., Wallentin, M., Kringelbach, M.L., & Vuust, P. Syncopation,  
718 body-movement and pleasure in groove music. *PloS One* **9**, e94446;  
719 10.1371/journal.pone.0094446 (2014).
- 720 29. Matthews, T.E., Witek, M.A., Heggli, O.A., Penhune, V.B., & Vuust, P. The sensation  
721 of groove is affected by the interaction of rhythmic and harmonic complexity. *PloS One*  
722 **14**, e0204539; (2019).
- 723 30. Konvalinka, I., Vuust, P., Roepstorff, A., & Frith, C.D. Follow you, follow me:  
724 continuous mutual prediction and adaptation in joint tapping. *Quarterly Journal of*  
725 *Experimental Psychology* (2006) **63**, 2220-30; 10.1080/17470218.2010.497843 (2010).
- 726 31. Heggli, O.A., Konvalinka, I., Kringelbach, M.L., & Vuust, P. Musical interaction is  
727 influenced by underlying predictive models and musical expertise. *Scientific Reports* **9**,  
728 1-13; (2019).
- 729 32. Pecenka, N., & Keller, P.E. The role of temporal prediction abilities in interpersonal  
730 sensorimotor synchronization. *Experimental Brain Research* **211**, 505-15;  
731 10.1007/s00221-011-2616-0 (2011).
- 732 33. Vuust, P., & Kringelbach, M.L. The pleasure of making sense of music.  
733 *Interdisciplinary science reviews* **35**, 166-182; (2010).
- 734 34. Gebauer, L., Kringelbach, M.L., & Vuust, P. Ever-changing cycles of musical pleasure:  
735 The role of dopamine and anticipation. *Psychomusicology: Music, Mind, and Brain* **22**,  
736 152; (2012).
- 737 35. Brattico, E., & Pearce, M. The neuroaesthetics of music. *Psychology of Aesthetics,  
738 Creativity, and the Arts* **7**, 48; (2013).
- 739 36. Alluri, V., Toiviainen, P., Jaaskelainen, I.P., Glerean, E., Sams, M., & Brattico, E.  
740 Large-scale brain networks emerge from dynamic processing of musical timbre, key  
741 and rhythm. *NeuroImage* **59**, 3677-89; 10.1016/j.neuroimage.2011.11.019 (2012).

- 742 37. Burunat, I., Alluri, V., Toivainen, P., Numminen, J., & Brattico, E. Dynamics of brain  
743 activity underlying working memory for music in a naturalistic condition. *Cortex* **57**,  
744 254-69; 10.1016/j.cortex.2014.04.012 (2014).
- 745 38. Bonetti, L., Brattico, E., Carlomagno, F., Cabral, J., Stevner, A., Deco, G., Whybrow,  
746 P.C., Pearce, M., Pantazis, D., & Vuust, P. Spatiotemporal brain dynamics during  
747 recognition of the music of Johann Sebastian Bach. *bioRxiv*, (2020).
- 748 39. Bonetti, L., Brattico, E., Bruzzone, S.E.P., Donati, G., Deco, G., Pantazis, D., Vuust, P.,  
749 & Kringelbach, M.L. Temporal pattern recognition in the human brain: a dual  
750 simultaneous processing. *bioRxiv*, (2021).
- 751 40. Bonetti, L., Brattico, E., Carlomagno, F., Donati, G., Cabral, J., Haumann, N.T., Deco,  
752 G., Vuust, P., & Kringelbach, M.L. Rapid encoding of musical tones discovered in  
753 whole-brain connectivity. *NeuroImage* **245**, 118735;  
754 10.1016/j.neuroimage.2021.118735 (2021).
- 755 41. Serra, J., Corral, A., Boguna, M., Haro, M., & Arcos, J.L. Measuring the evolution of  
756 contemporary western popular music. *Scientific Reports* **2**, 521; 10.1038/srep00521  
757 (2012).
- 758 42. Mencke, I., Quiroga-Martinez, D.R., Omigie, D., Michalareas, G., Schwarzacher, F.,  
759 Haumann, N.T., Vuust, P., & Brattico, E. Prediction under uncertainty: Dissociating  
760 sensory from cognitive expectations in highly uncertain musical contexts. *Brain  
761 Research* **1773**, 147664; 10.1016/j.brainres.2021.147664 (2021).
- 762 43. Vuvan, D.T., Podolak, O.M., & Schmuckler, M.A. Memory for musical tones: the  
763 impact of tonality and the creation of false memories. *Frontiers in Psychology* **5**, 582;  
764 10.3389/fpsyg.2014.00582 (2014).
- 765 44. Ockelford, A., & Sergeant, D. Musical expectancy in atonal contexts: Musicians'  
766 perception of "antistructure". *Psychology of Music* **41**, 139-174; (2013).
- 767 45. Mencke, I., Omigie, D., Wald-Fuhrmann, M., & Brattico, E. Atonal Music: Can  
768 Uncertainty Lead to Pleasure? *Frontiers in Neuroscience* **12**, 979;  
769 10.3389/fnins.2018.00979 (2018).
- 770 46. Daynes, H. Listeners' perceptual and emotional responses to tonal and atonal music.  
771 *Psychology of Music* **39**, 468-502; (2011).
- 772 47. Nieminen, S., Istók, E., Brattico, E., & Tervaniemi, M. The development of the  
773 aesthetic experience of music: preference, emotions, and beauty. *Musicae Scientiae* **16**,  
774 372-391; (2012).

- 775 48. Proverbio, A.M., Manfrin, L., Arcari, L.A., De Benedetto, F., Gazzola, M.,  
776 Guardamagna, M., Lozano Nasi, V., & Zani, A. Non-expert listeners show decreased  
777 heart rate and increased blood pressure (fear bradycardia) in response to atonal music.  
778 *Frontiers in Psychology* **6**, 1646; 10.3389/fpsyg.2015.01646 (2015).
- 779 49. Krumhansl, C.L., & Cuddy, L.L., *A theory of tonal hierarchies in music*, in *Music*  
780 *perception*. 2010, Springer. p. 51-87.
- 781 50. Taulu, S., & Simola, J. Spatiotemporal signal space separation method for rejecting  
782 nearby interference in MEG measurements. *Physics in Medicine and Biology* **51**, 1759-  
783 68; 10.1088/0031-9155/51/7/008 (2006).
- 784 51. Penny, W.D., Friston, K.J., Ashburner, J.T., Kiebel, S.J., & Nichols, T.E., *Statistical*  
785 *parametric mapping: the analysis of functional brain images*. 2011: Elsevier.
- 786 52. Oostenveld, R., Fries, P., Maris, E., & Schoffelen, J.M. FieldTrip: Open source  
787 software for advanced analysis of MEG, EEG, and invasive electrophysiological data.  
788 *Computational Intelligence and Neuroscience* **2011**, 156869; 10.1155/2011/156869  
789 (2011).
- 790 53. Woolrich, M.W., Jbabdi, S., Patenaude, B., Chappell, M., Makni, S., Behrens, T.,  
791 Beckmann, C., Jenkinson, M., & Smith, S.M. Bayesian analysis of neuroimaging data  
792 in FSL. *NeuroImage* **45**, S173-86; 10.1016/j.neuroimage.2008.10.055 (2009).
- 793 54. Mantini, D., Della Penna, S., Marzetti, L., de Pasquale, F., Pizzella, V., Corbetta, M., &  
794 Romani, G.L. A signal-processing pipeline for magnetoencephalography resting-state  
795 networks. *Brain Connectivity* **1**, 49-59; 10.1089/brain.2011.0001 (2011).
- 796 55. Gross, J., Baillet, S., Barnes, G.R., Henson, R.N., Hillebrand, A., Jensen, O., Jerbi, K.,  
797 Litvak, V., Maess, B., Oostenveld, R., Parkkonen, L., Taylor, J.R., van Wassenhove,  
798 V., Wibral, M., & Schoffelen, J.M. Good practice for conducting and reporting MEG  
799 research. *NeuroImage* **65**, 349-63; 10.1016/j.neuroimage.2012.10.001 (2013).
- 800 56. Bonetti, L., Haumann, N.T., Vuust, P., Kliuchko, M., & Brattico, E. Risk of depression  
801 enhances auditory Pitch discrimination in the brain as indexed by the mismatch  
802 negativity. *Clinical Neurophysiology* **128**, 1923-1936; 10.1016/j.clinph.2017.07.004  
803 (2017).
- 804 57. Bonetti, L., Haumann, N.T., Brattico, E., Kliuchko, M., Vuust, P., Sarkamo, T., &  
805 Naatanen, R. Auditory sensory memory and working memory skills: Association  
806 between frontal MMN and performance scores. *Brain Research* **1700**, 86-98;  
807 10.1016/j.brainres.2018.06.034 (2018).

- 808 58. Bonetti, L., Bruzzone, S.E.P., Sedghi, N.A., Haumann, N.T., Paunio, T., Kantojarvi, K.,  
809 Kliuchko, M., Vuust, P., & Brattico, E. Brain predictive coding processes are associated  
810 to COMT gene Val158Met polymorphism. *NeuroImage* **233**, 117954;  
811 10.1016/j.neuroimage.2021.117954 (2021).
- 812 59. Kroese, D.P., Taimre, T., & Botev, Z.I. Handbook of Monte Carlo Methods. John  
813 Wiley & Sons. Inc., Hoboken, New Jersey, (2011).
- 814 60. Huang, M.X., Mosher, J.C., & Leahy, R.M. A sensor-weighted overlapping-sphere  
815 head model and exhaustive head model comparison for MEG. *Physics in Medicine and*  
816 *Biology* **44**, 423-40; 10.1088/0031-9155/44/2/010 (1999).
- 817 61. Brookes, M.J., Stevenson, C.M., Barnes, G.R., Hillebrand, A., Simpson, M.I., Francis,  
818 S.T., & Morris, P.G. Beamformer reconstruction of correlated sources using a modified  
819 source model. *NeuroImage* **34**, 1454-65; 10.1016/j.neuroimage.2006.11.012 (2007).
- 820 62. Hillebrand, A., & Barnes, G.R. Beamformer analysis of MEG data. *International*  
821 *Review of Neurobiology* **68**, 149-71; 10.1016/S0074-7742(05)68006-3 (2005).
- 822 63. Lewicki, M.S. Efficient coding of natural sounds. *Nature Neuroscience* **5**, 356-63;  
823 10.1038/nn831 (2002).
- 824 64. Norman-Haignere, S.V., Kanwisher, N., McDermott, J.H., & Conway, B.R. Divergence  
825 in the functional organization of human and macaque auditory cortex revealed by fMRI  
826 responses to harmonic tones. *Nature Neuroscience* **22**, 1057-1060; 10.1038/s41593-  
827 019-0410-7 (2019).
- 828 65. Hackett, T.A. Anatomic organization of the auditory cortex. *Handbook of Clinical*  
829 *Neurology* **129**, 27-53; 10.1016/B978-0-444-62630-1.00002-0 (2015).
- 830 66. Mashour, G.A., Roelfsema, P., Changeux, J.-P., & Dehaene, S. Conscious processing  
831 and the global neuronal workspace hypothesis. *Neuron* **105**, 776-798; (2020).
- 832 67. Dehaene, S., Kerszberg, M., & Changeux, J.-P. A neuronal model of a global  
833 workspace in effortful cognitive tasks. *Proceedings of the national Academy of*  
834 *Sciences* **95**, 14529-14534; (1998).
- 835 68. Dehaene, S., & Naccache, L. Towards a cognitive neuroscience of consciousness: basic  
836 evidence and a workspace framework. *Cognition* **79**, 1-37; 10.1016/s0010-  
837 0277(00)00123-2 (2001).
- 838 69. Dehaene, S., & Changeux, J.P. Experimental and theoretical approaches to conscious  
839 processing. *Neuron* **70**, 200-27; 10.1016/j.neuron.2011.03.018 (2011).